

## Old Dominion University ODU Digital Commons

Electrical & Computer Engineering Faculty  
Publications

Electrical & Computer Engineering

1998

# Surface Morphology of Laser-Superheated Pb(111) and Pb(100)


Z. H. Zhang  
*Old Dominion University*

Bo Lin  
*Old Dominion University*

X. L. Zeng  
*Old Dominion University*

H. E. Elsayed-Ali  
*Old Dominion University*, [helsayed@odu.edu](mailto:helsayed@odu.edu)

Follow this and additional works at: [https://digitalcommons.odu.edu/ece\\_fac\\_pubs](https://digitalcommons.odu.edu/ece_fac_pubs)

 Part of the [Condensed Matter Physics Commons](#), and the [Electrical and Computer Engineering Commons](#)

### Repository Citation

Zhang, Z. H.; Lin, Bo; Zeng, X. L.; and Elsayed-Ali, H. E., "Surface Morphology of Laser-Superheated Pb(111) and Pb(100)" (1998). *Electrical & Computer Engineering Faculty Publications*. 107.  
[https://digitalcommons.odu.edu/ece\\_fac\\_pubs/107](https://digitalcommons.odu.edu/ece_fac_pubs/107)

### Original Publication Citation

Zhang, Z. H., Lin, B., Zeng, X. L., & Elsayed-Ali, H. E. (1998). Surface morphology of laser-superheated Pb(111) and Pb(100). *Physical Review B*, 57(15), 9262-9269. doi:10.1103/PhysRevB.57.9262

This Article is brought to you for free and open access by the Electrical & Computer Engineering at ODU Digital Commons. It has been accepted for inclusion in Electrical & Computer Engineering Faculty Publications by an authorized administrator of ODU Digital Commons. For more information, please contact [digitalcommons@odu.edu](mailto:digitalcommons@odu.edu).

## Surface morphology of laser-superheated Pb(111) and Pb(100)

Z. H. Zhang, Bo Lin, X. L. Zeng, and H. E. Elsayed-Ali\*

*Department of Electrical and Computer Engineering, Old Dominion University, Norfolk, Virginia 23529*

(Received 3 October 1997; revised manuscript received 16 January 1998)

The surface step density on the vicinal Pb(111) and the surface vacancy density on Pb(100) after laser superheating and melting are investigated using reflection high-energy electron diffraction. With  $\sim 100$ -ps laser pulses, Pb(111) surface superheating does not significantly change the density of the steps and step-edge roughness. However, after laser surface melting, the average terrace width and the string length at the step edge become as large as those at room temperature. The average terrace width at 573 K changes from  $38 \pm 15$  to  $64 \pm 19$  Å after laser surface melting, while the average string length at the step edge changes from  $90 \pm 14$  to  $250 \pm 38$  Å. For Pb(100), the surface vacancy density remains unchanged when the surface is superheated without melting. However, when the laser fluence is high enough to cause surface melting, the surface vacancy density increases. This increase in vacancy density is attributed to fast diffusion of atoms in the liquid film formed on Pb(100) during laser melting. [S0163-1829(98)02316-9]

### I. INTRODUCTION

Superheating of solids is rarely observed due to the presence of a thin disordered surface layer formed below the melting point  $T_m$ , which provides a nucleation site for melting.<sup>1</sup> Premelting is particularly evident in open surfaces. For example, Pb(110) disorders at a temperature as low as 150 K below  $T_m = 600.7$  K, while Pb(111) remains ordered up to  $T_m - 0.05$  K.<sup>2,3</sup> The terrace width on Pb(111) depends on temperature and was observed to suddenly increase above 580 K.<sup>4</sup> Some surfaces that do not premelt have been observed to superheat under certain conditions.<sup>5-8</sup> Superheating of Pb{111} bounded microcrystallites by a few degrees above  $T_m$  was observed.<sup>5</sup> Superheating of Pb(111) and Bi(0001) and some superheating of Pb(100) by  $\sim 180$ -ps laser pulses was observed in time-resolved reflection high-energy electron diffraction (RHEED) experiments.<sup>6-8</sup> The Pb(111) and Bi(0001) surfaces superheat up to  $\sim 120$  and  $\sim 90$  K above  $T_m$  of Pb and Bi, respectively. Evidence of residual order on Pb(100) up to  $\sim 15$  K above  $T_m$  was also observed.<sup>7</sup> In contrast, the open Pb(110) surface premelts for similar laser heating conditions.<sup>9</sup> Molecular-dynamics (MD) simulations of surface melting of several fcc metals showed good agreement with the experimentally observed superheating of Pb(111).<sup>10,11</sup> One of these simulations showed that cooperative movement of the superheated surface atoms results in the filling of vacancies and the surface becomes atomically flat by a superheating surface repair process.<sup>11</sup> This annealing mechanism was attributed to the high vibrational amplitudes that atoms are forced into by the ultrafast superheating pulse.

We have investigated surface step density on Pb(111) and vacancy density on Pb(100) after laser superheating using RHEED.<sup>12,13</sup> We used similar experimental conditions as those previously used in time-resolved RHEED experiments on superheating of Pb(111) and Pb(100).<sup>6</sup> The present experiments were initiated to investigate the proposed surface annealing by superheating.<sup>11</sup> By carefully analyzing the RHEED intensity profile for Pb(111), the average surface step terrace size can be obtained.<sup>12,13</sup> Pb(111) maintained at

573 K,  $T_m = 600.7$  K, was heated by a laser with a pulse width of  $\sim 100$  ps measured at full width at half maximum (FWHM). Pb(111) surface superheating does not significantly change the density of the steps and step-edge roughness. After laser melting, we find that the average terrace width and the average string length at the step edge increase and become as large as those at room temperature. The terrace width is defined as the distance of a flat surface between an up and a down pair of steps. The string length is the length of a straight line of atoms at a step edge, bounded by up and down atomic steps at the edge. A sudden increase in terrace width is observed when the laser fluence is high enough to cause surface melting.

The Pb(100) surface undergoes vacancy-induced disordering, as observed using high-resolution low-energy electron diffraction (HRLEED).<sup>14</sup> By analyzing the RHEED background intensity, the surface vacancy density change can be estimated.<sup>13,15,16</sup> The generation of a high vacancy density at the surface results in an increased RHEED background intensity.<sup>16</sup> Changes in the step terrace width are observed as changes in the RHEED intensity profile.<sup>13,15</sup> Pb(100) maintained at 533 K was further heated by a pulsed laser with a pulse width of  $\sim 100$  ps measured at FWHM. When the laser pulses cause surface superheating without melting, we observed that the RHEED background intensity does not significantly change when compared to that before laser heating. This indicates that the surface vacancy density does not change after superheating. However, when the laser fluence is high enough to cause surface melting, the background intensity increases, indicating that the vacancy density is increased on the surface after laser melting.

### II. EXPERIMENTAL METHODS

The experiment was performed in an ultrahigh vacuum system with a base pressure less than  $7 \times 10^{-11}$  Torr. The electron-beam energy used for RHEED was 9 keV. A 6.4-mm-diam, 2-mm-thick Pb(111) and Pb(100) single crystals were chemically polished and sputtered clean at 520 K using a (1.5–2)-keV argon ion beam. After sputtering and anneal-

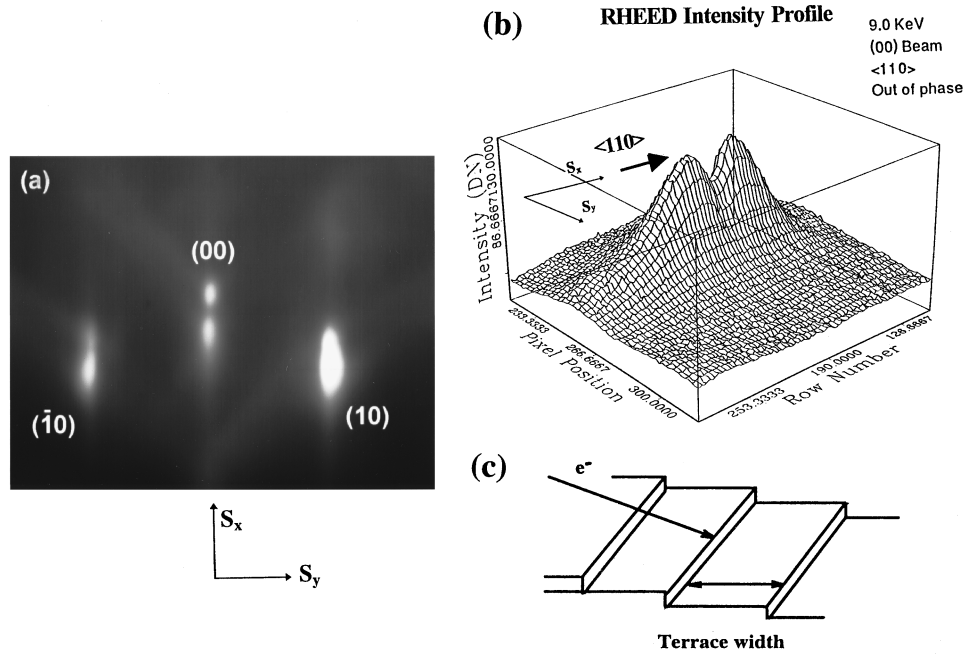


FIG. 1. (a) A RHEED pattern taken of the clean Pb(111)-1 $\times$ 1 surface at room temperature with an electron energy of 9 keV incident along the [110] direction. The angle of incidence of the electron beam is  $\sim 4.1^\circ$ , corresponding to the out-of-phase condition.  $S_x$  and  $S_y$  are the components of the momentum transfer parallel and perpendicular to the electron beam, respectively. (b) A RHEED intensity profile of the (00) beam. The average vicinal terrace width on Pb(111) at room temperature is  $85 \pm 25$  Å. The average string length at the vicinal step edge at room temperature is  $220 \pm 33$  Å. (c) A schematic illustration of vicinal steps.

ing the sample at 500 K for more than 10 hours, the Auger spectrum did not show any detectable impurity and we obtained a sharp 1 $\times$ 1 RHEED pattern of the Pb(111) and Pb(100) surfaces, which is acquired by a charge coupled device image acquisition system. A temperature uncertainty of  $\pm 2$  K near the Pb melting point and  $\pm 1$  K near the boiling point of water is estimated. Temperature stability within  $\pm 0.1$  K was attained using a temperature controller. A Nd:YAG (where YAG denotes yttrium aluminum garnet) laser operating at a wavelength  $\lambda = 1.06$   $\mu\text{m}$  and a pulse width of  $\sim 100$  ps with a 50-Hz repetition rate was used to heat the sample. The temperature rise of the Pb(111) and Pb(100) surfaces due to laser pulse irradiation was calculated from a one-dimensional heat diffusion model.<sup>17</sup> The error bar in the fluence is mainly due to the estimated spatial nonuniformity in the heating laser, measured to be 18% over the surface areas of the Pb(111) and Pb(100) crystals. This measurement was accomplished by scanning the laser beam by a  $\sim 100$ - $\mu\text{m}$  pinhole and therefore does not account for microscopic nonuniformity in the laser spatial profile. The laser peak fluence heating Pb(111) was varied from  $1.65$  to  $8.2 \times 10^7$  W/cm<sup>2</sup>. The laser peak fluence for Pb(100) was varied from  $0.4$  to  $10.6 \times 10^7$  W/cm<sup>2</sup>. The laser pulse causes a calculated peak  $\Delta T$  of  $22 \pm 4$  K for the  $(1.0 \times 10^7)$ -W/cm<sup>2</sup> peak laser fluence for both Pb(111) and Pb(100) since all parameters used in the calculation for both surfaces are the same.

### III. EXPERIMENTAL RESULTS

#### A. Pb(111)

Figure 1(a) is a RHEED pattern taken of the clean Pb(111)-1 $\times$ 1 surface obtained at room temperature with an electron energy of 9 keV incident along the [110] direction.

The angle of incidence of the electron beam was  $\sim 4.1^\circ$ , corresponding to the out-of-phase condition, in which the (00) beam profile is sensitive to surface steps or islands.  $S_x$  and  $S_y$  are the components of the momentum transfer parallel and perpendicular to the electron beam, respectively. Figure 1(b) is a three-dimensional RHEED intensity profile of the (00) beam in which a splitting producing two peaks along the [110] direction of the Pb crystal is observed. This indicates that surface steps are vicinal and perpendicular to the [110] direction, as schematically shown in Fig. 1(c).<sup>13,15</sup> The vicinal (111) surface means the surface is miscut from the (111) direction. This miscut surface has (111) terraces and steps of height of one or more atomic layers, the step edge being perpendicular to the [110] direction, as determined in our experiment. The spacing between the two split peaks along the [110] direction is  $0.246 \pm 0.07$  Å<sup>-1</sup>. Taking into account the instrumental response of  $0.172$  Å<sup>-1</sup>, the vicinal terrace width of the studied Pb(111) surface obtained at room temperature is  $85 \pm 25$  Å. The instrumental response is obtained from the FWHM of the (00) beam at the in-phase condition.<sup>18–20</sup> The intensity profile perpendicular to the [110] direction gives information on kinks and meanders at the step edge. Meanders refer to a turning or winding of the step at its edge, increasing the step-edge roughness. Fitting the intensity profile of the (00) beam to a Lorentzian function, a FWHM of  $0.142 \pm 0.02$  Å<sup>-1</sup> was obtained. Thus the measured average string length at the vicinal step edge obtained at room temperature is  $220 \pm 33$  Å. An instrumental response of  $0.114$  Å<sup>-1</sup> is used for the direction perpendicular to the electron beam. When the surface temperature is increased, the splitting in the peak becomes broad, indicating that the terrace width is decreased. Upon heating the surface above 543 K, the splitting in the peak disappeared and the

peak profile became a Lorentzian. This is due to either an increased randomness in terrace width or meandering at step edges, in particular, near  $T_m$ .<sup>13</sup> The measured average terrace width and average string length at 573 K decrease to  $42 \pm 17$  and  $70 \pm 11$  Å, respectively. Above 573 K, they continue to decrease up to 590 K, indicating that the vicinal Pb(111) surface undergoes a roughening transition at step edges due to the thermally generated meandering at step edges causing the observed changes in the average terrace width and string length and the disappearance of the splitting peak.

We next describe the change in surface step density of Pb(111) after laser superheating. The sample was heated from 323 to 573 K in  $\sim 10$  min. A total of 1000 laser pulses were used for each irradiation condition and laser heating was performed while the sample was kept at 573 K. This number of laser pulses was used to establish equilibrium conditions for surface roughness for a particular laser fluence as will be discussed later. The sample was then cooled back to 323 K in  $\sim 45$  min. Upon cooling back to 323 K followed by heating to 573 K, the average terrace width became nearly the same as that prior to laser treatment. This temperature recycling after laser irradiation allowed us to bring back the surface to nearly the same surface roughness conditions prior to each laser treatment. The FWHM of the (00) beam intensity profiles parallel and perpendicular to the [110] direction of the Pb crystal was measured at the out-of-phase condition before and after laser heating. The average surface terrace width and the average string length at the step edge is obtained after accounting for the instrumental response. Figure 2(a) shows that the average terrace width before and after laser heating does not change significantly below a laser fluence of  $[(6.2 \pm 1.1) \times 10^7]$ -W/cm<sup>2</sup> pulse energy. Above that laser fluence, the average terrace width increases from  $\sim 38$  to  $\sim 64$  Å for a laser energy of  $(8.2 \pm 1.5) \times 10^7$  W/cm<sup>2</sup>, becoming about the same width as that at room temperature. After laser heating at each fluence, the sample was cooled to 323 K and then thermally heated again to 573 K. This cooling of the sample followed by heating to 573 K results in a terrace width of  $\sim 40$  Å. Figure 2(b) shows the measured average string length before and after laser heating, which is an average of all lines of atoms at the step edge, as schematically shown in the inset. Below a laser peak fluence of  $\sim 6.2 \times 10^7$  W/cm<sup>2</sup>, the average string length is not affected by laser heating. Above that fluence, for example, the average string length changes from 90 to  $\sim 250$  Å for a laser peak fluence of  $8.2 \times 10^7$  W/cm<sup>2</sup>. At 573 K, even after laser heating, we did not observe a splitting peak as observed at room temperature, which means that the surface terrace width remains random or that the surface undergoes faceting even though meandering at step edges is decreased [Fig. 2(b)].

Based on kinematic diffraction, we conclude that these FWHM changes in the RHEED profiles are completely due to changes in step density and step-edge roughness, not vacancies.<sup>15,16</sup> From the RHEED profiles, we obtain the average terrace width and string length. Without taking into account the instrumental broadening, the RHEED intensity from a two-dimensional monatomic stepped surface produces a diffuse intensity in the shape of a Lorentzian function with the FWHM depending on step density.<sup>13,15</sup> For a

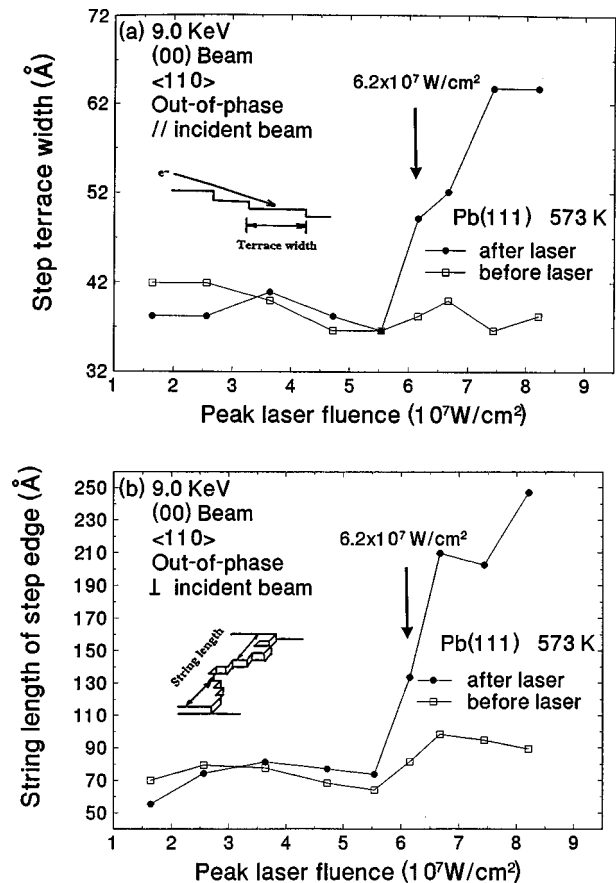


FIG. 2. (a) The average terrace width after laser heating remains almost unchanged for a laser peak fluence of  $(6.2 \pm 1.1) \times 10^7$  W/cm<sup>2</sup> and increases for higher fluences. It changes from  $\sim 38$  to  $\sim 64$  Å for a laser peak fluence of  $8.2 \times 10^7$  W/cm<sup>2</sup>, becoming about the same width as that at room temperature. The average terrace width before laser heating is shown to be  $\sim 40$  Å. (b) The average string length after laser heating increases above a laser peak fluence of  $\sim 6.2 \times 10^7$  W/cm<sup>2</sup> and changes from  $\sim 90$  to  $\sim 250$  Å above  $8.2 \times 10^7$  W/cm<sup>2</sup>.

vicinal stepped surface, the diffuse intensity is more complicated and gives a splitting shape.<sup>15</sup> If the surface is two dimensional containing only vacancies, an increase in the vacancy density causes the background intensity to increase without a broadening of the RHEED profile. For Pb(111), FWHM changes were observed, indicating that the step model applies to high-temperature disorder of Pb(111). This analysis is based upon the fact that dynamic and other effects do not significantly change the peak widths of RHEED profiles in our results. The dynamic effects and nonlinear surface effects such as a surface resonance do not in general cause the splitting of the peak below 543 K, as seen in Fig. 1. Upon heating the surface above 543 K, the splitting in the peak disappeared and the peak profile became a Lorentzian profile widths, in our experiment we measured the temperature dependence of the FWHM of the Lorentzian profile between 543 and 590 K at different out-of-phase conditions. The dynamic effects are dependent on the incident angle of the electron beam relative to the surface since these effects result from multiple interactions of all scattering layers.<sup>12</sup> However, we observed that the temperature dependence of

the average terrace width and string length is about the same for the different incident angles. Therefore, we conclude that the kinematic theory is applicable to our study of surface roughness.

For heating with a laser fluence less than  $6.2 \times 10^7 \text{ W/cm}^2$ , we do not observe a noticeable change in the average terrace width or string length. According to our heat diffusion model, the maximum surface temperature rise due to the  $\sim(6.2 \times 10^7)\text{-W/cm}^2$ , 100-ps laser pulse is  $136 \pm 30 \text{ K}$  above  $T_m$ . Previous time-resolved RHEED experiments on Pb(111) showed that the maximum superheating temperature was  $\sim 120 \text{ K}$ .<sup>6</sup> This measurement was performed with an  $\sim 180\text{-ps}$  FWHM laser and did not account for convolution effects arising from the electron pulse having a width about the same as the laser heating the surface. These convolution effects reduce the observed superheating. Considering convolution effects,  $\pm 18\%$  estimated nonuniformity of the laser heating, the uncertainties in the values of the different parameters in the calculation model, and the shorter laser pulse used in the present experiments, we conclude that the maximum superheating is reached for an  $\sim(6.2 \times 10^7)\text{-W/cm}^2$  laser peak fluence. At higher fluences, the surface melts. Thus superheating of Pb(111) without subsequent melting does not lead to a noticeable annealing of surface steps. For laser pulse fluences sufficient to cause melting after superheating, a sudden increase in the average terrace width and the average string length is observed.

The results in Fig. 2 were obtained for surface treatment with 1000 laser pulses. Surface roughness was strongly dependent on the number of laser pulses heating the surface at a particular fluence. Figure 3 shows the changes in the average terrace width and string length with the number of laser pulses used for a laser energy of  $\sim 6.8 \times 10^7 \text{ W/cm}^2$ , which causes surface melting. The changes in both the average terrace width and the average string length reach equilibrium after surface exposure to  $\sim 500$  laser pulses. After  $\sim 2000$  laser pulses, the average terrace width and string length decrease, indicating that surface damage starts to occur. This could be due to microscopic hot spots in the laser heating pulse causing accumulated laser damage to the surface. For a laser fluence below that required for melting, surface roughness is not affected. For surface heating with a single laser pulse, we did not observe any change in the average terrace width and string length for laser peak fluences up to  $\sim 8.2 \times 10^7 \text{ W/cm}^2$ .

In a MD simulation of superheating of Cu(111), a vacancy annealing mechanism, repairing the surface through superheating, was proposed based on a non-diffusional cooperative movement of surface atoms.<sup>11</sup> In that model, superheating of Cu(111) by 40 K above  $T_m$  was observed, while Cu(110) melted. Even a highly damaged Cu(111) surface, with as much as 10% preexisting vacancies, could also be superheated. This is surprising: Since melting nucleates at defects, a highly defective surface is not expected to superheat. In this mechanism, however, a high density of vacancy clusters is annealed by the action of adlayer islands that embed locally into the topmost layer. The surface became atomically flat. This surface annealing mechanism is thought to be a result of the high vibrational amplitudes that atoms are forced into by the ultrafast superheating pulse. For Pb(111), our results show that superheating, by itself, does

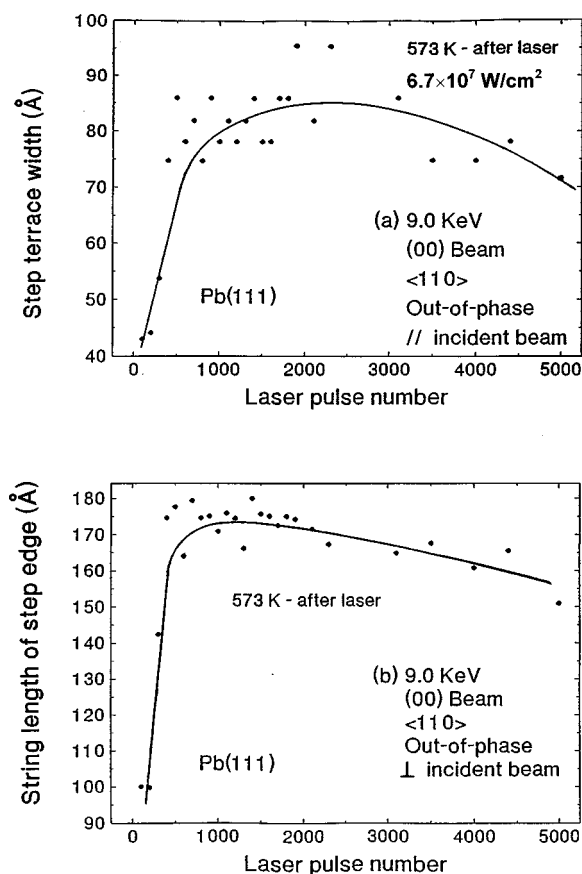


FIG. 3. Changes in the average terrace width and string length with the number of heating laser pulses for a laser peak fluence of  $\sim 6.7 \times 10^7 \text{ W/cm}^2$ , which causes surface melting. (a) Average terrace width. (b) Average string length.

not anneal surface steps. When the threshold for superheating is exceeded and surface melting occurs, a significant reduction in step density and average string length on these steps is observed after a number of laser pulses. Van Pinxteren, Pluis, and Frenken observed that for Pb(111), surface-melting-induced faceting occurs at high temperatures.<sup>3</sup> If the surface is misoriented with respect to the (111) orientation, the surface decomposes at high temperatures into dry and melted facets with a variety of orientations. In our experiment, the fact that the split in the (00) RHEED peak profile was not observed at 573 K after laser surface melting, even though there was a large increase in the average step width and string length, could be explained by facet formation. Faceting of the vicinal Pb(111) was reported in the MD simulation of Bilalbegović, Ercolessi, and Tosatti.<sup>21</sup> At room temperature, the vicinal Pb(111) is a monatomic stepped surface, while at  $T=0.97T_m$  it becomes a (111) facet and a tilted melted surface. Facets with five monatomic step height with a variety of orientations, between  $18^\circ$  and  $27^\circ$  away from the (111) orientation, produce a large step terrace. The broadening terrace width is approximately 1.67 times the terrace width of a monatomic step at room temperature. The equilibration time for the formation of a facet is  $\sim 1 \text{ ns}$ . The temperature for surface-melting-induced faceting in our experiments should be higher than that estimated in the MD simulation, 583 K, since we did not observe a thermally sudden increase in the terrace width up to 590 K.<sup>22</sup> For a

laser fluence above the surface melting threshold, facet formation can occur after surface melting. With each laser shot of  $\sim 100$  ps FWHM, the surface is heated above the melting threshold for  $\sim 150$  ps, in which the mobility of surface atoms is much higher than that for the solid.<sup>23</sup> During that time, the facets can easily grow. After each laser pulse, defaceting is slow because the sample is maintained at 573 K, close to a temperature at which faceting occurs.<sup>3,21</sup> Subsequent laser pulses make the facets grow even further. After  $\sim 400$  laser pulses with an energy of  $\sim 6.7 \times 10^7$  W/cm<sup>2</sup> the facet size reaches an equilibrium (Fig. 3). The equilibrium terrace width after 400 pulses becomes  $\sim 80$  Å, about twice the terrace width prior to laser melting, which is consistent with the factor of 1.67 obtained from the MD simulation.<sup>21</sup> The change in the terrace width is  $\sim 40$  Å; therefore, the growth rate of a terrace is  $\sim 0.1$  Å per pulse. For a single laser pulse, the change in the terrace width,  $\sim 0.1$  Å, is too small to observe. By cooling the sample to room temperature and then heating it up to 573 K, the terrace width becomes about the same as that prior to laser treatment. This is because at low temperature, the facet is not stable and defaceting occurs faster than that at 573 K. For a laser fluence sufficient to cause surface superheating without melting, the mobility of surface atoms remains small, consistent with that for a solid surface. Therefore, the terrace width does not change and the surface is not annealed.

We note that the MD simulation on superheating of Cu(111) dealt only a perfectly oriented (111) surface with some adatom-vacancy clusters.<sup>11</sup> Our Pb(111) surface is a stepped surface cut off the perfect (111) orientation. It is well known that step edges act as sinks of atomic-size defects, making the adatom diffusion strongly anisotropic, and the annealing of such defects depends on whether long terrace edges are available nearby. This could explain the lack of annealing by superheating in our experiment that was performed on a vicinal Pb(111) surface. In addition, the latest MD simulation of Bilalbegović, Ercolessi, and Tosatti showed that the (111) surface is isotropic, the large surface stress is built up in the superheating regime, and anomalous layer relaxation and vibrational amplitudes exit during superheating.<sup>24</sup>

### B. Pb(100)

We next discuss the effect of  $\sim 100$ -ps FWHM laser superheating and melting of Pb(100). Figure 4(a) shows the (00) beam peak intensity as a function of temperature at the in-phase and out-of-phase conditions. The angles of incidence of the electron beam along the [011] direction of the Pb crystal at the in-phase and out-of-phase conditions were  $\sim 2.1^\circ$  and  $3.0^\circ$ , respectively. In this figure, the intensity at the in-phase condition decreases with temperature almost exponentially below 480 K and deviates gradually from the exponential Debye-Waller dependence above 480 K. The Debye-Waller factor  $2M = wT$  and below 480 K corresponds to a slope  $w = 0.01034$  K<sup>-1</sup>. The angular profiles of the (00) beam at the out-of-phase condition at room temperature parallel and perpendicular to the incident direction of the electron beam, the [011] direction of the Pb single crystal, correspond to Lorentzian profiles, indicating that surface steps are monatomic in height.<sup>13</sup> We did not observe any split peaks in the (00) beam as was observed for Pb(111), which

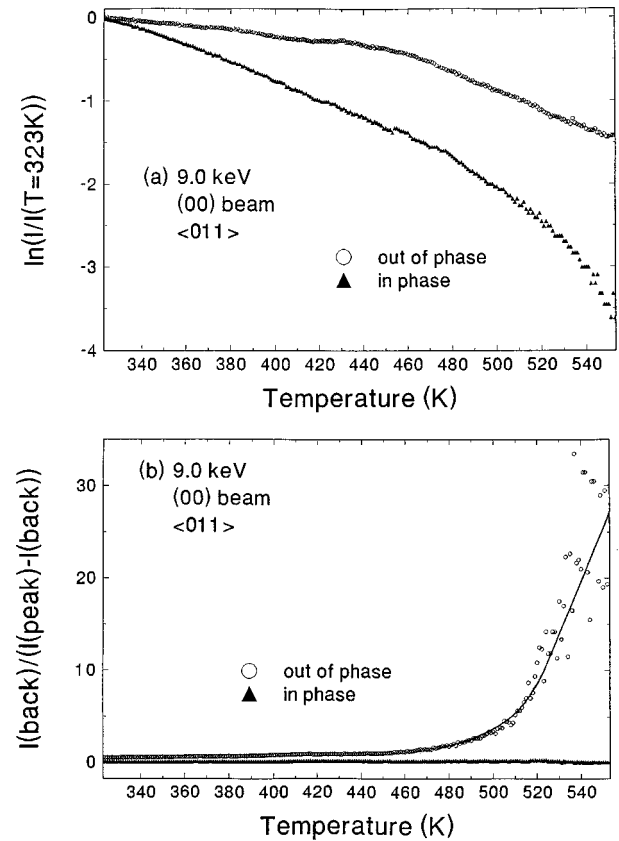


FIG. 4. (a) Peak intensity changes in the (00) beam as a function of temperature at the in-phase and out-of-phase conditions. The angles of incidence of the electron beam along the [011] direction of the Pb crystal at the in-phase and out-of-phase conditions were  $\sim 2.1^\circ$  and  $\sim 3.0^\circ$ , respectively. (b) The background intensity changes with temperature show significant changes in the background intensity above 480 K at the out-of-phase condition.

indicates that the Pb(100) surface steps are not vicinal.<sup>13</sup> The FWHM of the RHEED profile parallel to the incident direction of the electron beam at this out-of-phase condition is  $0.13$  Å<sup>-1</sup>, which is the same width as that experimentally obtained at the in-phase condition. This suggests that the experimentally measurement precision is about  $\delta = \pm 0.01$  Å<sup>-1</sup>, so that the step terrace width is wider than the  $2\pi/\delta = 628$  Å instrumental resolution.<sup>15,18,20</sup> With increasing temperature, we did not observe any change in the FWHM of the RHEED profile at the out-of-phase condition, indicating that the step terrace width does not change with temperature. Figure 4(b) shows that the background intensity changes with temperature at both the in-phase and out-of-phase conditions. We observed significant changes in the background intensity with temperature above 480 K at the out-of-phase condition. In this figure,  $I_{\text{peak}}$  is the (00) peak intensity and  $I_{\text{back}}$  is the background intensity. The background intensity is normalized to the peak intensity by calculating the ratio  $R = I_{\text{back}}/(I_{\text{peak}} - I_{\text{back}})$ . This normalized background  $R$  is obtained at  $0.20$  Å<sup>-1</sup>, which is about 11% of the first Brillouin zone. The increase in the measured background intensity above 480 K at the out-of-phase condition reveals that the surface develops a high density of vacancies, in agreement with the HRLEED observations.<sup>14</sup>

We investigated the change in the RHEED background intensity after laser heating. The sample was kept at 533 K

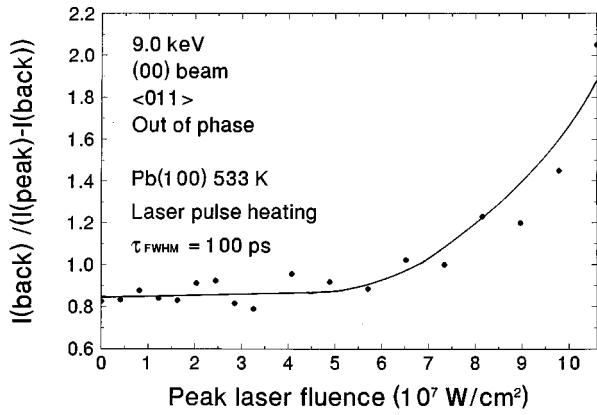


FIG. 5. Change in the ratio  $R = I_{\text{back}} / (I_{\text{peak}} - I_{\text{back}})$  as a function of peak laser fluence for heating with 1000 laser pulses at each fluence.  $I_{\text{back}}$  is the RHEED background intensity, while  $I_{\text{peak}}$  is the (00) peak intensity. The ratio  $R$  does not change below a peak laser fluence of  $6.5 \times 10^7 \text{ W/cm}^2$ . Above that fluence, the background significantly increases.

using a hot stage while the laser pulses were used to transiently heat the surface. Figure 5 shows the change in the ratio  $R = I_{\text{back}} / (I_{\text{peak}} - I_{\text{back}})$  as a function of peak laser fluence for heating with 1000 laser pulses at each fluence. The ratio  $R$  does not change below a peak laser fluence of  $6.5 \times 10^7 \text{ W/cm}^2$ . Above that fluence, the background significantly increases. In addition, we did not observe any change in the FWHM of the (00) beam profile parallel and perpendicular to the [011] direction of the Pb crystal indicating that the step density does not change after laser heating.

The temperature rise on the Pb(100) surface due to the laser heating pulse is calculated by a one-dimensional heat diffusion model.<sup>6,17</sup> The error bar in the fluence is mainly due to the estimated nonuniformity in the heating laser beam profile, which was measured to be 18% across the surface. The laser peak fluence was varied from  $0.4$  to  $10.6 \times 10^7 \text{ W/cm}^2$ . A peak temperature rise of  $22 \pm 4 \text{ K}$  for the  $1.0 \times 10^7 \text{ W/cm}^2$  laser peak fluence was calculated using a heat diffusion model. The bulk melting point  $T_m$  is  $600.7 \text{ K}$  and the previously measured maximum superheating temperature  $T_{\text{super}}$  is  $\sim 635 \text{ K}$ . Above  $T_{\text{super}} \sim 635 \text{ K}$ , the laser fluence is high enough to cause the surface to melt. This temperature corresponds to a peak laser fluence of  $\sim 4.8 \times 10^7 \text{ W/cm}^2$ . From Fig. 5 we conclude that laser superheating of Pb(100) does not cause any noticeable change in the RHEED background intensity. When the surface is heated beyond the maximum superheating temperature, the surface melts and a sharp increase in the RHEED background intensity is observed.

Based on kinematics diffraction, for a two-dimensional surface containing only vacancies, the background intensity increases with the vacancy density without broadening the RHEED profile.<sup>13,14,20</sup> The ratio  $R = I_{\text{back}} / (I_{\text{peak}} - I_{\text{back}})$  can be determined by  $R \propto [(2n - 1)^{-2} - 1] (1 + 2M)$  for the out-of-phase condition,<sup>14</sup> where  $2M = wT$  is the Debye-Waller factor,  $w = 0.01034 \text{ K}^{-1}$  is the measured slope in our experiment, and  $n$  is the surface vacancy density. Therefore, the vacancy density is given by  $n \propto \frac{1}{2} [R / (1 + 2M) + 1]^2 + \frac{1}{2}$ . The vacancy density change is  $\Delta n = n/n_0 - 1$ , where  $n_0$  is the initial vacancy density before heating. From Fig. 4(b), we

calculate the  $\sim 20\%$  increase in vacancy density at  $480 \text{ K}$  from that at  $323 \text{ K}$ . At  $530 \text{ K}$ ,  $\Delta n$  increases by  $\sim 300\%$ , indicating a higher generation of vacancy density in our case than that previously observed in HRLEED experiments in which the measured increase in vacancy density was  $(20 \pm 5)\%$  at  $530 \text{ K}$  from its value at room temperature.<sup>14</sup> The observed larger increase in the vacancy density in our case may be related to the different initial surface vacancy density at room temperature due to the different surface sputter treatment conditions in the two experiments. Both experiments, however, show that the change in the vacancy density increases exponentially with temperature and that large concentrations of vacancies are created above  $510 \text{ K}$ . From Fig. 5 we obtain the vacancy density change as a function of peak laser fluence. The vacancy density is almost constant below  $6.5 \times 10^7 \text{ W/cm}^2$  and increases up to about  $20\%$  above  $10.0 \times 10^7 \text{ W/cm}^2$  due to surface melting.

The results show that laser superheating of Pb(100) does not anneal surface vacancies. In a MD simulation of ultrafast laser heating of Cu(111), large concentrations of vacancies and adatoms were shown to anneal through a nondiffusional cooperative mechanism in which the adatoms settle in the top layer, while the cooperative atom movement results in the filling of vacancies.<sup>11</sup> The experimentally observed stability of the surface vacancy density may be due to the relatively low rate of surface diffusion of atoms on the solid Pb(100) surface. The surface diffusion of atoms was measured for Pb(110) and was estimated from a molecular-dynamic simulations for Au(100), Au(111), and Au(110).<sup>23,25</sup> The one-dimensional diffusion coefficient below the melting point for Au(100) is estimated to be  $\sim 1.0 \times 10^{-6} \text{ cm}^2/\text{s}$ . In our experiment, we used  $\sim 100$ -ps laser pulses, which raises the surface temperature above  $T_m$  for  $100$ – $150 \text{ ps}$ . Within such a time scale, the atom diffusion length is  $\sim 1$ – $2 \text{ \AA}$ , which is less than the  $4.95$ - $\text{\AA}$  lattice constant of Pb(100). Thus surface adatoms do not diffuse enough to fill existing vacancies. On the other hand, the one-dimensional diffusion constant above the melting point for Au(100) is  $\sim 2.5 \times 10^{-5} \text{ cm}^2/\text{s}$ , resulting in a diffusion length on a time scale of  $100 \text{ ps}$  much larger than the lattice constant of Pb(100). Such a large diffusion rate of adatoms on the surface causes the filling of vacancies. In the thin liquid film during surface melting, vacancies are also generated. If the rate of vacancy generation is higher than that of filling vacancies during laser melting, the vacancy density is increased. As a result, the surface vacancy density increases with the number of laser pulses and with the peak laser fluence. In contrast, Pb(111) is a stepped surface and shows that surface faceting occurs after laser melting, producing about twice the terrace width prior to laser melting.

Figure 6 shows the dependence of the ratio  $R$  on the number of laser pulses used to heat the surface for a peak laser fluence of  $7.34 \times 10^7 \text{ W/cm}^2$ , sufficient to melt the surface. The RHEED background intensity clearly increases up to 1500 pulses. The calculated result from Fig. 6 shows that vacancy density is increased from its starting point by  $\sim 20\%$  after 1000 laser pulses. The vacancy density is seen to slightly decrease as the number of heating laser pulses is increased beyond  $\sim 1500$  pulses. A possible reason is that the generation of vacancies due to melting tends to saturate; thus the rate of filling vacancies due to large adatom diffusion

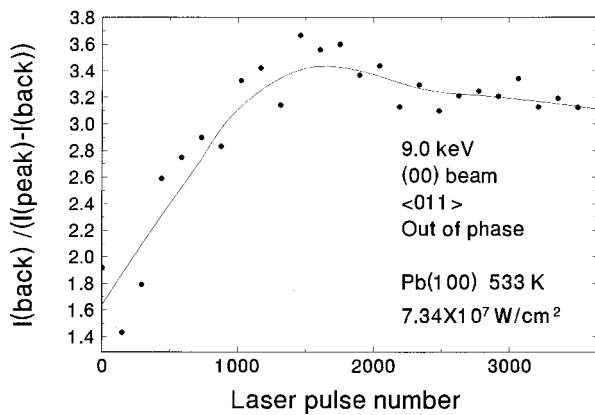


FIG. 6. Dependence of the ratio  $R$  on the number of laser pulses used to heat the surface for a peak laser fluence of  $7.34 \times 10^7 \text{ W/cm}^2$ , sufficient to melt the surface. The RHEED background intensity increases up to  $\sim 1500$  pulses.

becomes higher than generating vacancies. Therefore, the vacancy density is slightly decreased in contrast to that below 1500 pulses. In the present experiment, we did not observe any change in the surface step density as observed in our work on vicinal Pb(111) where we observed that the surface step density is largely decreased after surface melting. Molecular-dynamics simulations of fcc(100) shows a weak disorder only in the first atomic layer and the surface does not undergo faceting.<sup>25</sup> The lack of faceting for fcc(100) surfaces appears to be related to the high temperature for disordering of the two uppermost layers of the flat (100) surface.<sup>21,25</sup> In medium-energy ion scattering experiments, the disordered layer thickness on Pb(100) was observed to saturate at 1.3 monolayers, measured up to  $T_m - 0.05 \text{ K}$ .<sup>26</sup> A

periodic density modulation in the disordered layer in a direction parallel to the disordered layer interface is thought to make the disordered layer stable against further melting.<sup>27</sup>

#### IV. CONCLUSION

For Pb(111) heated with  $\sim 100$ -ps laser pulses, superheating does not significantly change the average step width or the step edge roughness. A sudden increase in terrace width is achieved only when the laser fluence is high enough to cause surface melting. The average terrace width and the average string length at the step edge become as large as those at room temperature. The average terrace width at 573 K for a peak laser fluence of  $8.2 \times 10^7 \text{ W/cm}^2$  changes from  $38 \pm 15$  to  $64 \pm 19 \text{ \AA}$  after laser heating, while the average string length at the step edge changes from  $90 \pm 14$  to  $250 \pm 38 \text{ \AA}$ .

For Pb(100), after laser superheating, with a laser fluence below the melting threshold, we observed that the RHEED background intensity does not significantly change compared to that before laser heating. Thus surface vacancy density does not change after superheating. When the laser fluence is high enough to cause surface melting, we observed an increase in the background intensity, indicating an increase in the surface vacancy density. This increase in vacancies maybe attributed to the larger diffusion of atoms in the liquid film on Pb(100) during laser melting.

#### ACKNOWLEDGMENT

This work was supported by the U.S. Department of Energy, under Grant Nos. DE-FG05-93ER45504 and DE-FG02-97ER45625.

\*Author to whom correspondence should be addressed. FAX: (757) 683-3220. Electronic address: elsayed-ali@ece.odu.edu

<sup>1</sup>D. P. Woodruff, *The Solid-Liquid Interface* (Cambridge University Press, London, 1973).

<sup>2</sup>J. W. M. Frenken and J. F. van der Veen, *Phys. Rev. Lett.* **54**, 134 (1985).

<sup>3</sup>B. Pluis, A. W. Denier van der Gon, J. W. M. Frenken, and J. F. Van der Veen, *Phys. Rev. Lett.* **59**, 2678 (1987); H. M. Van Pinxteren, B. Pluis, and J. W. M. Frenken, *Phys. Rev. B* **49**, 13 798 (1994).

<sup>4</sup>H. N. Yang, T. M. Lu, and G. C. Wang, *Phys. Rev. Lett.* **62**, 2148 (1989).

<sup>5</sup>J. J. Métois and C. Heyraud, *Ultramicroscopy* **31**, 73 (1989); *J. Phys. (Paris)* **50**, 3175 (1989); Z. H. Zhang, P. Kulatunga, and H. E. Elsayed-Ali, *Phys. Rev. B* **56**, 4141 (1997).

<sup>6</sup>J. W. Herman and H. E. Elsayed-Ali, *Phys. Rev. Lett.* **69**, 1228 (1992); *Phys. Rev. B* **49**, 4886 (1994).

<sup>7</sup>J. W. Herman, H. E. Elsayed-Ali, and E. A. Murphy, *Phys. Rev. Lett.* **71**, 400 (1993).

<sup>8</sup>E. A. Murphy, H. E. Elsayed-Ali, and J. W. Herman, *Phys. Rev. B* **48**, 4921 (1993).

<sup>9</sup>J. W. Herman and H. E. Elsayed-Ali, *Phys. Rev. Lett.* **68**, 2952 (1992).

<sup>10</sup>F. D. Di Tolla, F. Ercolessi, and E. Tosatti, *Phys. Rev. Lett.* **74**, 3201 (1995).

<sup>11</sup>H. Häkkinen and Uzi Landman, *Phys. Rev. Lett.* **71**, 1023 (1993).

<sup>12</sup>S. Ino, *Jpn. J. Appl. Phys.* **16**, 891 (1977); M. A. Van Hove and C. M. Chen, *Low Energy Electron Diffraction* (Springer-Verlag, Berlin, 1989).

<sup>13</sup>M. G. Lagally, D. E. Savage, and M. C. Tringides, in *Reflection High-Energy Electron Diffraction and Reflection Imaging of Surfaces*, Vol. 188 of *NATO Advanced Study Institute Series B: Physics*, edited by K. Larson and P. J. Dobson (Plenum, New York, 1988), p. 139.

<sup>14</sup>H.-N. Yang, K. Fang, G.-C. Wang, and T.-M. Lu, *Phys. Rev. B* **44**, 1306 (1991).

<sup>15</sup>C. S. Lent and P. I. Cohen, *Surf. Sci.* **139**, 121 (1984).

<sup>16</sup>J. M. Pimbley and T. M. Lu, *Surf. Sci.* **139**, 360 (1984).

<sup>17</sup>H. E. Elsayed-Ali and J. W. Herman, *Appl. Phys. Lett.* **57**, 1508 (1990).

<sup>18</sup>J. M. Van Hove and P. I. Cohen, *J. Vac. Sci. Technol. A* **1**, 609 (1983).

<sup>19</sup>H. N. Yang, T. M. Lu, and G. C. Wang, *Phys. Rev. Lett.* **62**, 2148 (1989).

<sup>20</sup>T. M. Lu and M. G. Lagally, *Surf. Sci.* **99**, 695 (1980).

<sup>21</sup>G. Bilalbegović, F. Ercolessi, and E. Tosatti, *Europhys. Lett.* **17**, 333 (1992).

<sup>22</sup>Yang *et al.* observed a sudden increase in terrace width at 580 K in HRLEED experiments,<sup>4</sup> which may be related to the difference in the surface morphology between the crystals used. The surface steps at room temperature in the experiment of



- Yang *et al.* show randomness in its terrace width since no splitting peak was observed, in contrast to the vicinal surface observed in our case.
- <sup>23</sup>J. W. M. Frenken, J. P. Toennies, and Ch. Wöll, Phys. Rev. Lett. **60**, 1727 (1988).
- <sup>24</sup>G. Bilalbegović, Phys. Rev. B **55**, 16 450 (1997).
- <sup>25</sup>H. Häkkinen and M. Manninen, Phys. Rev. B **46**, 1725 (1992).
- <sup>26</sup>H. M. Van Pinxteren and J. W. M. Frenken, Surf. Sci. **275**, 383 (1992).
- <sup>27</sup>A. A. Chernov and L. V. Mikheev, Phys. Rev. Lett. **60**, 2488 (1988); A. A. Chernov and L. V. Mikheev, Physica A **157**, 1042 (1989).